

# On the Feasibility of Detecting Quantized Conductance in Neutral Matter

Yuki Sato, Byeong-Ho Eom, and Richard Packard

Department of Physics, University of California, Berkeley, CA 94720-7300, USA  
E-mail: ysato@socrates.berkeley.edu

(Received May 18, 2005; revised July 18, 2005)

*When an electrochemical potential difference (i.e., a voltage) is applied across a metal wire whose transverse dimensions are on the order of the electron's Fermi wavelength, the conductance  $G \equiv I/\Delta V$  becomes quantized in units of  $2e^2/h$ . We present calculations that show that when a chemical potential difference  $\Delta\mu_3$  is applied across an array of small apertures whose sizes are comparable to the Fermi wavelength of  $^3\text{He}$  in a  $^3\text{He}:\text{}^4\text{He}$  mixture, the mass conductance  $G \equiv \left(\frac{I_3}{\Delta\mu_3/m_3^*}\right)$  will be quantized in units of  $2m_3^{*2}/h$  where  $m_3^*$  is the  $^3\text{He}$  effective mass. We show that the mass conductance will be quantized for a 0.1% mixture passing through 10 nm diameter pores at temperatures below 25 mK. The phenomenon should be observable in a filter material made by nuclear track etching.*

**KEY WORDS:** conductance; Fermi wavelength; quasiparticle; ballistic transport.

## 1. INTRODUCTION

Electron transport properties in mesoscopic conductors have been studied for almost two decades. Various experiments<sup>1-6</sup> have shown that electrical conductance through a narrow constriction can be quantized in units of  $2e^2/h$ . This is interpreted as a consequence of quantized transverse momentum in the channel using the Landaur formulation.<sup>7,8</sup>

The key ingredients necessary for the observation of quantized conductance are (1) degenerate Fermions, (2) a path whose dimension is comparable to the Fermi wavelength, and (3) ballistic transport.

It is natural to ask if these conditions can be met and analogous phenomena observed in neutral matter, free of electron repulsions. One

might imagine sending a degenerate Fermi fluid through an aperture whose transverse dimensions are comparable to the Fermi wavelength of that particular atom, and finding the mass conductance to be quantized. A material that should exhibit this phenomenon is  ${}^3\text{He}$  which is a degenerate fluid at temperatures below  $\approx 0.5$  K. However, the Fermi wavelength for pure  ${}^3\text{He}$  is  $\approx 0.7$  nm. It is very difficult to prepare a tube or aperture of that size even with the best nano-fabrication techniques available today. In addition, it is a misperception to view matter as a liquid when traveling in channels comparable to the atomic size.

In this paper, we show that one can use a dilute mixture of  ${}^3\text{He}$ - ${}^4\text{He}$  to study this quantum transport. The magnitudes indicate that the mass conductance will be quantized and the effect should be observable.

## 2. DERIVATION OF QUANTIZED MASS CONDUCTANCE

In this section, we show that the mass conductance will be quantized for  ${}^3\text{He}$  dissolved in superfluid  ${}^4\text{He}$  by treating  ${}^3\text{He}$  atoms as delocalized Fermi quasiparticles in the background of  ${}^4\text{He}$ . Imagine two reservoirs of  ${}^3\text{He}$ - ${}^4\text{He}$  mixture connected with a small channel (see Fig. 1).

The work necessary to move one  ${}^3\text{He}$  particle from reservoirs 1–2 is  $\Delta\mu_3$ , which is the chemical potential difference across the channel for a single  ${}^3\text{He}$  particle. We assume here that the mixture is dilute enough that  ${}^3\text{He}$ - ${}^3\text{He}$  interactions are negligible compared to  ${}^3\text{He}$ - ${}^4\text{He}$  hydrodynamic interactions. In this limit, we reduce the effect of  ${}^4\text{He}$  background to the renormalization of  ${}^3\text{He}$  bare mass.

We first solve the problem for a simple case where the channel can be viewed as a one-dimensional path. In this extreme case, one can write the mass current as  $n_3 m_3^* v$ , where the number density  $n_3$  can be approximated as the density of states at the Fermi level  $D(E_F)$  times the excitation energy  $\Delta\mu_3$ . Then,

$$\begin{aligned} I_3 &\approx D(E_F) \Delta\mu_3 m_3^* v_F \\ &= \frac{2m_3^*}{h p_F} \Delta\mu_3 m_3^* \frac{p_F}{m_3^*} \\ &= \frac{2m_3^*}{h} \Delta\mu_3. \end{aligned} \quad (1)$$

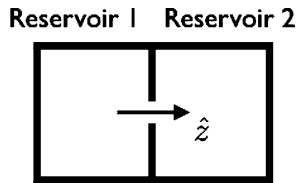


Fig. 1. Mass flow through a channel.

Therefore, if we define the mass conductance,  $G$ , to be the mass current divided by the chemical potential per unit mass

$$G = \frac{I_3}{\Delta\mu_3/m_3^*} = \frac{2m_3^{*2}}{h}. \tag{2}$$

We now do the same treatment for a more generalized three-dimensional channel whose cross-sectional area is given by  $\Delta x \Delta y$ . Having this constricted geometry in the  $x$ - $y$  plane in real space means that one can only define states as small as  $\Delta p_x \Delta p_y$  in corresponding directions in momentum space with relations such as  $\Delta p_x \cdot \Delta x \approx h$ .

We excite the system with  $\Delta\mu_3$  to create mass current, which gives rise to a shell of width  $\Delta p$  around the Fermi sphere (see Fig. 2). The particles that are within this shell are the ones that can be involved in the transport. Using the argument above with this quasiparticle picture, the smallest state definable in the shell is shown as the hatched region, and its size can be written as  $\Delta p_x \Delta p_y (\Delta p / \cos \theta)$ . This state is what is often referred to as the “channel” in momentum space and it plays the role of a quantum in conductance. If the excitation energy,  $\Delta\mu_3$ , is small compared to the Fermi energy, the number density of particles in the hatched volume is

$$n \approx D(E_F) \times \Delta\mu_3 \times \frac{(\Delta p_x \Delta p_y)(\Delta p / \cos \theta)}{4\pi p_F^2 \Delta p}. \tag{3}$$

Then the mass current contribution from this single “channel” in momentum space is

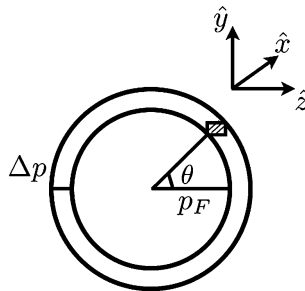


Fig. 2. Fermi sphere.

$$\begin{aligned}
I_z &= (n \cdot m_3^*) (\vec{v} \cdot \hat{z}) (\Delta x \Delta y) \\
&\approx \left\{ D(E_F) \times \Delta \mu_3 \times \frac{(\Delta p_x \Delta p_y) (\Delta p / \cos \theta)}{4\pi p_F^2 \Delta p} \right\} m_3^* (v_F \cos \theta) (\Delta x \Delta y) \\
&\approx \left\{ \frac{8\pi m_3^* p_F}{h^3} \times \Delta \mu_3 \times \frac{(\hbar^2 / \Delta x \Delta y) (\Delta p / \cos \theta)}{4\pi p_F^2 \Delta p} \right\} m_3^* \left( \frac{p_F}{m_3^*} \cos \theta \right) (\Delta x \Delta y) \\
&= \frac{2m_3^*}{h} \Delta \mu_3. \tag{4}
\end{aligned}$$

Therefore, as in the one-dimensional case,

$$G = \frac{I_3}{\Delta \mu_3 / m_3^*} = \frac{2m_3^{*2}}{h}. \tag{5}$$

As one increases the physical channel size  $\Delta x \Delta y$  in real space,  $\Delta p_x \Delta p_y$  decreases, and more “channels” in momentum space open up. If there are  $n$  of them contributing, then the conductance is  $nG_0$  where  $G_0 \equiv (2m_3^{*2}/h)$ .

### 3. HOW TO APPROACH QUANTUM LIMIT

The quantum modifications to transport occur when the channel dimensions are comparable to the wavelength of the carriers. In the electron case, one can fabricate nano-size devices to match the electron wavelength. However, in the case of  ${}^3\text{He}$ , we cannot take that approach because the Fermi wavelength is simply too small. Some natural silicates such as Zeolites have three-dimensional frameworks that form narrow channels of extremely uniform size ( $\approx 0.5$  nm) but such materials are not variable by the experimenter. Rather than seeking smaller channels, one may take the opposite approach which is to find a fluid whose Fermi wavelength matches the smallest apertures obtainable.  ${}^3\text{He}$ : ${}^4\text{He}$  mixtures are a natural choice. The main focus of this paper is to address the question: Is there a parameter range (concentration, Fermi wavelength, Fermi temperature, aperture size, current magnitude, surface reflectivity, etc.) that will permit observation of quantized conductance in neutral matter?

At low enough temperatures, liquid  ${}^3\text{He}$  in superfluid  ${}^4\text{He}$  behaves as an ideal Fermi gas with an effective mass  $m_3^*$ . For dilute mixtures, the  ${}^3\text{He}$  concentration  $\chi \equiv n_3 / (n_3 + n_4) \approx n_3 / n_4$ .

The Fermi wavelength is a function of  ${}^3\text{He}$  concentration,<sup>9</sup>

$$\lambda_F \approx \left( \frac{8\pi}{3} \right)^{\frac{1}{3}} \left( \frac{1}{\chi n_4} \right)^{\frac{1}{3}}. \tag{6}$$

We may imagine that  $\chi$  is a “knob” that can be turned to vary  $\lambda_F$ . Decreasing the concentration increases  $\lambda_F$ , but the Fermi temperature drops correspondingly.

$$T_F \approx \frac{\hbar^2}{2m_3^*k_B} \left(3\pi^2\chi n_4\right)^{\frac{2}{3}}. \quad (7)$$

To ensure complete degeneracy, one might strive for temperatures  $T \approx \frac{T_F}{10}$ . The smaller the concentration, the lower the temperature for quantum phenomena to appear.

Porous filters in the form of  $5\mu\text{m}$  thick sheets containing high density 10 nm size apertures made with nuclear track etching are commercially available.<sup>10</sup> Using  $m_3^* \approx 2.46m_3$ ,<sup>11</sup> a concentration of 0.1% gives  $\lambda_F \approx 7.3\text{ nm}$  and  $T_F \approx 25\text{ mK}$ . Millikelvin technology, especially nuclear adiabatic demagnetization, gives access to the temperature range around 1 mK where this mixture will be almost completely degenerate.

#### 4. BALLISTIC TRANSPORT

The last ingredient requires the  $^3\text{He}$  mean free path to be longer than the channel dimensions. We compute the quasiparticle mean free path from  $^3\text{He}$ - $^4\text{He}$  mixture viscosity. In a dilute solution of degenerate  $^3\text{He}$  in superfluid  $^4\text{He}$ , the viscosity is given by Meyerovich,<sup>12</sup> and Bashkin<sup>13</sup>

$$\eta = \frac{1}{24\pi^3} \frac{1}{(kT)^2} \frac{p_F^5}{a^2 m_3^{*2}} 0.81 = 0.81 \frac{1}{24\pi^3} \frac{(3\pi^2 n_4)^{\frac{5}{3}} \chi^{\frac{5}{3}}}{k^2 a^2 m_3^{*2} T^2}, \quad (8)$$

where  $a$  is the s-wave scattering length for the collision of two  $^3\text{He}$  quasiparticles. Then, using the relation  $l = \frac{5\eta}{n_3 p_F}$ ,

$$l = 0.81 \frac{5}{24\pi^3} \frac{(3\pi^2)^{\frac{4}{3}} n_4^{\frac{1}{3}}}{k^2 a^2 m_3^{*2}} \frac{1}{T^2} \chi^{\frac{1}{3}}. \quad (9)$$

This gives  $l \approx 30\mu\text{m}$  for  $\chi = 0.1\%$ ,  $a \approx -1.5\text{ \AA}$ ,<sup>14</sup> and  $T = 1\text{ mK}$ . Therefore, the mean free path is large compared to the channel length which is on the order of  $5\mu\text{m}$  for track-etched materials, and we expect the  $^3\text{He}$  to exhibit pure ballistic mass transport.

An important issue to address when dealing with ballistic propagation is the specularity on wall collisions. As one lowers the experimental temperature, the  $^3\text{He}$ - $^3\text{He}$  collision probability which scales as  $\left(\frac{T}{T_F}\right)^2$  decreases rapidly and the scattering at the wall starts to dominate over the quasiparticle scattering in the bulk.<sup>15,16</sup> If the wall is rough, collisions will

alter the component of particle momentum parallel to the surface and  $^3\text{He}$  quasiparticles will scatter diffusively. The detection of quantized conductance is therefore sensitive to the surface reflectivity of the flow channel.

One can estimate the effective smoothness of the wall by considering the ratio of the  $^3\text{He}$  Fermi wavelength  $\lambda_F$  to the characteristic size of the surface roughness  $R$ . This ratio is

$$\frac{\lambda_F}{R} \approx \frac{1}{R} \left( \frac{8\pi}{3\chi n_4} \right)^{\frac{1}{3}} \approx 7 \quad (10)$$

for  $\chi \approx 10^{-3}$  and  $R \approx 1$  nm, which indicates that the wall surface would be rough even with nano-scale inhomogeneities. However, in  $^3\text{He}$ - $^4\text{He}$  mixtures,  $^4\text{He}$  preferentially coats the wall due to its smaller zero-point motion and as a result enhances the surface specularly dramatically. It has been shown<sup>17-20</sup> that the scattering of  $^3\text{He}$  quasiparticles from walls coated with superfluid  $^4\text{He}$  is quasielastic and nearly 100% specular. This  $^4\text{He}$ -induced specularly is not due to the geometrical smoothing of inhomogeneities on the wall. What is important is the superfluidity of  $^4\text{He}$  that coats the surface. The degree of specularly increases rapidly after two monolayers of surface  $^4\text{He}$  (indicating the onset of  $^4\text{He}$  superfluidity) and it is well over 0.9 after five monolayers.<sup>20</sup> Therefore, using a mixture of  $^3\text{He}$ - $^4\text{He}$  should ensure that the scattering within the conduction path does not destroy the phase coherence of the quasiparticle matter wave.

We note that the fraction of  $^3\text{He}$  quasiparticles that can interact with the wall by propagating ballistically through the surface  $^4\text{He}$  layers decreases with increasing  $^4\text{He}$  thickness but should always stay finite. Although small, the effect that this might have on the system (such as wall-driven localization)<sup>21</sup> needs further investigation.

## 5. THE SIGNAL SIZE: DEGENERACY PRESSURE AND CONDUCTANCE CURRENT

If a chemical potential difference is applied across an aperture, a  $^3\text{He}$  quasiparticle mass current, proportional to  $\Delta\mu_3$  will result. Equation (5) predicts that the ratio  $G = \left( \frac{I_3}{\Delta\mu_3/m_3^*} \right)$  will be quantized in units of  $(2m_3^*/h)$ . In this section, we estimate the magnitude of the mass current resulting from typical values of  $\Delta\mu_3$  and compare it to the size of current that can presently be observed in experiments dealing with flow of cryogenic liquids. We find that the current from a single aperture is below observable limits but the current flowing through an array of many apertures will be detectable.

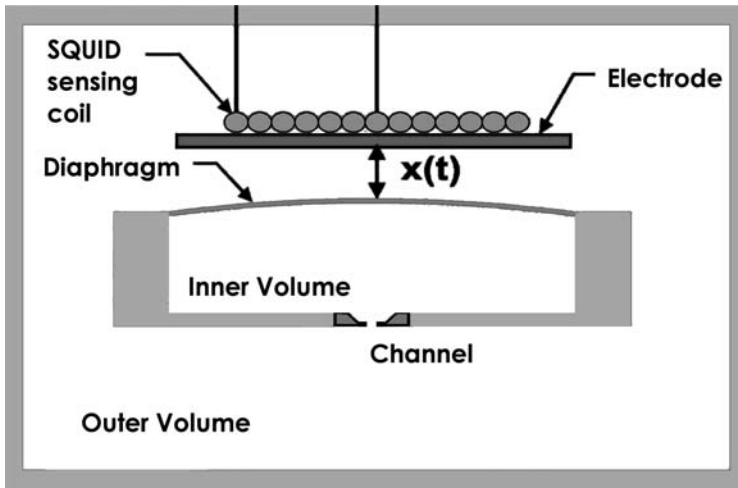


Fig. 3. A possible experimental setup.

Consider the apparatus sketched in Fig. 3. Two volumes filled with  $^3\text{He}$ : $^4\text{He}$  mixtures are separated by a diaphragm and a nano-scale diameter tube. A thin flexible diaphragm is coated with a superconducting film so that it can be pulled toward the electrode by applying a voltage between them. This creates a pressure difference  $\Delta P$  across the channel.  $\Delta P$  is related to the diaphragm displacement  $\Delta x$  by Hooke's Law;

$$\Delta P = -\frac{k\Delta x}{A}, \quad (11)$$

where  $A$  is the diaphragm area and  $k$  is the spring constant. The flow that results from this pressure head may be monitored by measuring the diaphragm position,  $x(t)$ , with a SQUID-based displacement sensor.<sup>22</sup> It has been shown that this type of transducer can measure displacement as small as  $10^{-15}$  m/ $\sqrt{\text{Hz}}$  (which corresponds to  $1 \mu\text{Pa}/\sqrt{\text{Hz}}$  in pressure) and current as small as  $5 \times 10^{-17}$  kg/sec.

The mass current that is measured has two components  $I_4$  and  $I_3$ .  $I_4$  is the superfluid  $^4\text{He}$  current and  $I_3$  is due to the normal  $^3\text{He}$ . It is the conductance for  $I_3$  that will be quantized. One needs to analyze the flow dynamics and untangle these two. This task can be simplified by comparing the time scales involved in each flow.

Unlike the normal fluid, the superfluid velocity through an aperture is almost independent of the pressure applied, limited by the intrinsic critical velocity  $\approx 10$  m/sec.<sup>23</sup> One can estimate the time scale associated with the superflow by dividing the displaced mass ( $\approx \rho_4 dV$ ) by the critical current.

With the typical volume of the experimental cell  $V \approx 1$  cc, one could electrostatically pull on the diaphragm and make a fractional volume change  $\frac{dV}{V} \approx 10^{-4}$ . Using the aperture area  $a = \pi(5 \text{ nm})^2 \approx 8 \times 10^{-17} \text{ m}^2$ , and the critical velocity  $v_c \approx 10 \text{ m/sec}$ ,  $t \approx dM_4/I_4 \approx \rho_4 dV/\rho_4 v_c a \approx 10^5 \text{ sec}$ . If a commercial porous filter<sup>10</sup> with a pore density of  $10^8/\text{cm}^2$  is used, a  $1 \text{ mm}^2$  sample will have  $10^6$  channels. Then the time scale for superflow becomes on the order of  $\approx 0.1 \text{ sec}$ . After this time, the superfluid should start to oscillate about its new equilibrium position. The resonant mode is determined by the restoring force of the diaphragm and the inertia of the moving fluid, and its quality factor can be extremely high at temperatures of our interest. However, one can actively damp this Helmholtz oscillation so that it will not overwhelm the signal from  $^3\text{He}$  flow.

As the superfluid  $^4\text{He}$  responds to the pressure head, a concentration difference is established across the apertures. Then the resultant osmotic pressure which approaches the Fermi degeneracy pressure in the low temperature limit drives the  $^3\text{He}$  quasiparticles. Using Eqs. (5) and (11),

$$I_3 = G \frac{\Delta\mu_3}{m_3^*} = G \frac{\Delta P_F}{\rho_3} = G \frac{(k\Delta x/A)}{\rho_3}. \quad (12)$$

The mass conservation requires  $I_3 = \rho\dot{x}A$ . These two relations give  $\Delta x \propto e^{-t/\tau}$  with  $\tau = (\rho\rho_3 A^2/kG)$ . Using the typical values of  $A \approx 1 \text{ cm}^2$ ,  $k \approx 3000$ , and  $\chi = 10^{-3}$  gives  $\tau \approx 6 \text{ min}$  for  $10^6$  apertures. Therefore, this time scale which is much longer than that for superfluid  $^4\text{He}$  should allow one to easily separate the  $^3\text{He}$  current from the  $^4\text{He}$ .

In Fermi degenerate systems,  $U = \frac{3}{5}NE_F$ . Then, the degeneracy pressure

$$P_F = -\frac{dU}{dV} = \frac{\hbar^2}{5m_3^*} \left(3\pi^2\right)^{\frac{2}{3}} n_3^{\frac{5}{3}}. \quad (13)$$

Making a fractional volume change ( $dV/V$ ) by moving the diaphragm corresponds to making a fractional number density change, and therefore the concentration change. Differentiating  $P$  with respect to the number density, and setting  $(dn/n) = (dV/V) = (d\chi/\chi)$ ,

$$\frac{\Delta\mu_3}{m_3^*} = \frac{\Delta P}{\rho_3} = \frac{1}{\rho_4} \left( \frac{\hbar^2}{3m_3^*} \left(3\pi^2\right)^{\frac{2}{3}} n_4^{\frac{5}{3}} \right) \chi^{\frac{2}{3}} \frac{d\chi}{\chi}. \quad (14)$$

This is the chemical potential difference per unit mass that is created across the aperture. Then, using Eq. (5), the resultant current for one

quantum of conductance is

$$dI_3 = G \frac{\Delta\mu_3}{m_3^*} = \frac{2m_3^{*2}}{h} \frac{1}{\rho_4} \left( \frac{\hbar^2}{3m_3^*} (3\pi^2)^{\frac{2}{3}} n_4^{\frac{5}{3}} \right) \chi^{\frac{2}{3}} \frac{d\chi}{\chi}. \quad (15)$$

For  $\chi = 10^{-3}$ ,  $\rho_3 \approx \rho_4 \cdot \chi$ ,  $m_3^* \approx 2.46m_3$ , and  $\frac{d\chi}{\chi} = 10^{-4}$ ,  $dI_3$  is  $\approx 1.5 \times 10^{-21}$  kg/sec per aperture. This is too small to observe. However, with  $10^6$  channels, the total current is  $\approx 1.5 \times 10^{-15}$  kg/sec, which can be measured with the displacement transducer described above.

One might wonder if it is problematic to introduce so many apertures. The size distribution rather than the number of channels might obscure the steps in conductance. If different channels have different transverse dimensions, the current contribution from each will overlap and “wash out” the steps. Just how sharp the size distribution has to be to observe quantized mass conductance is discussed in the simulation below.

The nature of the track etching process which employs exposing the membrane to a collimated charged particles and then etching the sensitized tracks should ensure a relatively narrow pore size distribution. However, it may not be a simple task to find the actual distribution. The track-etched filters are made of electrically insulating polycarbonate, which causes the sample to be charged and deflect the beam scans for SEM imaging. Their thickness ( $\approx 5 \mu\text{m}$ ) makes it difficult to obtain good transmittance for conventional TEM which requires the sample to be thinned down to a few 100-nm thickness.

## 6. SIMULATION

A plot of simulated mass conductance vs  $^3\text{He}$  concentration is shown in Fig. 4 with two different channel size distributions. The Fermi wavelength was calculated for a particular value of  $^3\text{He}$  concentration, and it was compared with the size of an aperture to determine its conductance. This was done for  $10^6$  apertures whose sizes had a Gaussian distribution with a peak at 10 nm and a specified standard deviation around that peak. This procedure was repeated for different values of  $\chi$  to produce this figure. The effect of channel size distribution is very apparent.

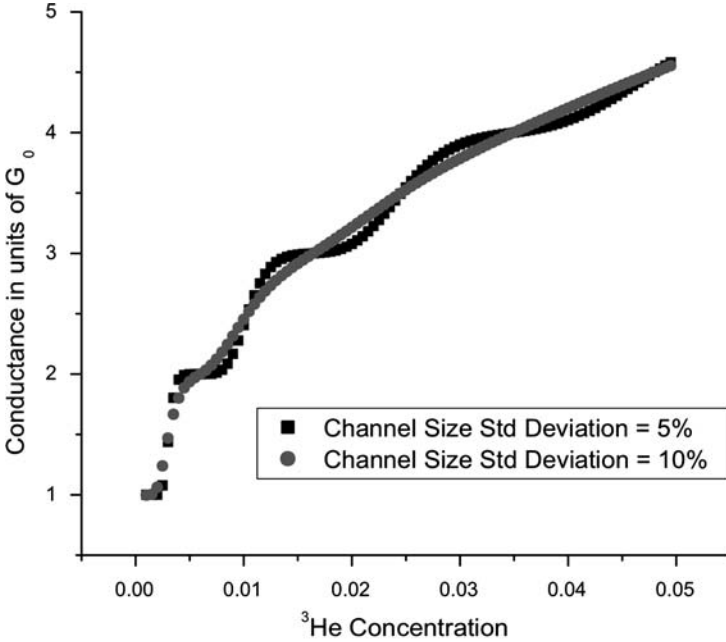


Fig. 4. Simulated mass conductance vs  $^3\text{He}$  concentration for 10 nm size channels. Conductance is plotted in units of  $G_0 \equiv 2m_3^*/h$ .

## 7. CONCLUSION

We have shown that when a chemical potential,  $\Delta\mu_3$ , is applied across an array of apertures whose dimensions are comparable to the Fermi wavelength of  $^3\text{He}$  in a  $^3\text{He}:$  $^4\text{He}$  mixture, the mass conductance  $G \equiv \left(\frac{I_3}{\Delta\mu_3/m_3^*}\right)$  will be quantized in units of  $2m_3^*/h$ . We predict this phenomenon will be observable in a 0.1% solution below 25 mK if track-etched filter materials with 10 nm size holes are used. Varying the  $^3\text{He}$  concentration should allow one to adjust the Fermi wavelength and observe the quantized steps in conductance.

## ACKNOWLEDGMENT

We are grateful to J. Spence, J. Wu, and J. Quispe for their microscopy work. We are also grateful for helpful discussions with K. Penanen, A. Meyerovich, and J. Moore. This work is supported in part by the NSF-DMR-0244882.

## REFERENCES

1. B. J. van Wees, L. P. Kouwenhoven, H. van Houten, C. W. J. Beenakker, J. E. Mooij, C. T. Foxton, and J. J. Harris, *Phys. Rev. B* **38**, 3625 (1988).
2. H. van Houten and C. Beenakker, *Phys. Today* **49**, 22 (1996).
3. B. J. van Wees, H. van Houten, C. W. J. Beenakker, J. G. Williamson, L. P. Kouwenhoven, D. van der Marel, and C. T. Foxon, *Phys. Rev. Lett.* **60**, 848 (1988).
4. E. Scheer, P. Joyez, D. Esteve, C. Urbina, and M. H. Devoret, *Phys. Rev. Lett.* **78**, 3535 (1997).
5. E. Scheer, N. Agrait, J. Carlos Cuevas, A. Levy Yeyati, B. Ludoph, A. Martin-Rodero, G. Rubio Bollinger, J. M. van Ruitenbeek, and C. Urbina, *Nature* **394**, 154 (1998).
6. J. L. Costa Kramer and N. Garcia, *Phys. Rev. B* **55**, 12910 (1997).
7. R. Landauer, *IBM J. Res. Rev.* **1**, 223 (1957).
8. R. Landauer, *J. Phys. Condens. Matt.* **1**, 8099 (1989).
9. G. Baym and C. Pethick, in *Physics of Liquid and Solid Helium*, K. H. Bennemann and J. B. Ketterson, eds., (1978), Wiley, Vol. 2, pp. 123–175.
10. SPI-Pore and Nuclepore brands Polycarbonate Membrane Filters.
11. J. Landau, J. T. Tough, N. R. Brubaker, and D. O. Edwards, *Phys. Rev. A* **2**, 2472 (1970).
12. A. E. Meyerovich, *Prog. Low Temp. Phys.* **11**, 1 (1987).
13. E. P. Bashkin, *Sov. Phys. JETP* **46**, 972 (1977).
14. E. P. Bashkin and A. E. Meyerovich, *Adv. Phys.* **30**, 1 (1981).
15. A. E. Meyerovich, *J. Low Temp. Phys.* **124**, 461 (2001).
16. A. E. Meyerovich and R. Jochemsen, *J. Low Temp. Phys.* **126**, 193 (2001).
17. D. A. Ritchie, J. Saunders, and D. F. Brewer, *Phys. Rev. Lett.* **59**, 465 (1987).
18. S. M. Tholen and J. M. Parpia, *Phys. Rev. Lett.* **68**, 2810 (1992).
19. M. R. Freeman, R. S. Germain, E. V. Thuneberg, and R. C. Richardson, *Phys. Rev. Lett.* **60**, 596 (1988).
20. S. M. Tholen and J. M. Parpia, *Phys. Rev. B* **47**, 319 (1993).
21. A. E. Meyerovich and S. Stepaniants, *Phys. Rev. B* **51**, 116 (1995).
22. H. J. Paik, *J. Appl. Phys.* **47**, 1168 (1976).
23. E. Varoquaux, M. W. Meisel, and O. Avenel, *Phys. Rev. Lett.* **57**, 18 (1986).